Comparisons of Linear Regression Models for Properties of Alkaliactivated Binder Concrete

Arkamitra Kar
Birla Institute of Technology and Science (BITS)

Udaya B. Halabe
West Virginia State College

Indrajit Ray
Indiana University-Purdue University Fort Wayne

Avinash Unnikrishnan
Portland State University

Citation Details

COMPARISONS OF LINEAR REGRESSION MODELS FOR PROPERTIES OF ALKALI-ACTIVATED BINDER CONCRETE

Arkamitra Kar
Birla Institute of Technology and Science - Pilani, Telangana, India
Udaya B. Halabe
West Virginia University, WV, USA
Indrajit Ray
Indiana University-Purdue University, IN, USA
Avinash Unnikrishnan
Portland State University, OR, USA

Abstract
Concrete with alkali-activated binder (AAB) is increasingly considered as a better alternative to conventional portland cement (PC) concrete due to its superior sustainable and green properties. In order to promote the practical usage of AAB concrete, a previous study by the present authors proposed models on correlations among their mechanical and nondestructive properties. The present study extends the previous knowledge by proposing new improved models using linear regressions to predict compressive strengths and modulus of elasticity from ultrasonic pulse velocities. The models are developed for both unstressed and stressed AAB concrete with different curing temperatures. The accuracies of the models are compared with both sum of squares due to errors (SSE) and R^2 depending on the type of equations; and the new models are found to be more accurate compared to the previous models.

Keywords: Alkali-activated concrete, Compressive strength, Modulus of Elasticity, Linear Regression models

Introduction
According to the World Business Council, 5 – 8% of the global carbon dioxide emissions are caused by the Portland cement (PC) concrete industry (Provis and van Deventer, 2009). The production of PC, therefore, contributes a large percentage of CO_2 out of the total carbon dioxide emissions. The PC production also consumes significant amount of natural

limestone and thus depletes the natural resources. Hence, an alternative binder material is needed to decrease the CO_2 emissions and save the natural resources. The binder materials must also possess adequate mechanical and structural properties comparable to PC. Alkali-activated binders (AABs) which can be produced by reaction of a precursor (fly ash or slag) and an activating solution (alkaline sodium silicate solution and sodium hydroxide mixture), is one such sustainable material. In 1979, Professor Davidovits of France produced this type of binders by mixing alkalis with burnt mixture of kaolinite, limestone and dolomite. He introduced the term ''geopolymer'' and also used several trademarks such as Pyrament, Geopolycem and Geopolymite for the binder (Davidovits 1994; Davidovits 2002). As a more generic material the name ''geopolymer'' is also popularly known as alkali-activated binder (AAB). Therefore the mixture of AAB and aggregates are known as AAB concrete. In order to apply this AAB concrete in real life conditions, it is important to develop effective correlations of their mechanical properties such as strength and modulus of elasticity with the nondestructive characteristics such as ultrasonic pulse velocity.

The primary goal of the paper is to refine the regression equations of the experimentally obtained compressive strength and modulus of elasticity values as functions of the ultrasonic pulse velocity for the AAB concrete presented in a previous study by same group of authors (Kar et al., 2013) and propose additional models. The set of equations proposed previously were based on theoretical approach and the proposed models involved regression through the origin. Although R^2 are popularly used as a measure of accuracy of models, the use of R^2 for these types of equations is questionable (Eisenhauer 2003). In this study, the accuracy of the proposed models are reevaluated on the basis of sum of squares due to errors (SSE). These regression equations can be used to predict the compressive strength and modulus of elasticity of group of AAB concrete using the ultrasonic pulse velocities as input parameter. Additional equations are developed including the intercepts and relative accuracies of the models with and without intercepts are compared to determine the efficient prediction equations of the modulus of elasticity and compressive strengths from ultrasonic pulse velocity. Equations were also generated to establish the relationship between the applied compressive stress and the corresponding ultrasonic velocities.

Materials and Testing Methods
Materials
Class F fly ash used in this study conforming to ASTM C618 (Standard Specification for Coal Fly Ash and Raw or Calcined Natural Pozzolan for Use in Concrete), was obtained from a local coal power plant.

2

The specific gravity, specific surface area and oxide composition are listed in Table 1 reproduced from Kar et al. (2013). Ground granulated blast furnace slag or slag conforming to Grade 100 of ASTM C989 (Standard Specification for Slag Cement for Use in Concrete and Mortars) obtained from local steel plant were used in this study (Table 1 reproduced from Kar et al., 2013). The coarse aggregate used was 12.5 mm graded and crushed limestone conforming to ASTM C33/C33M (Standard Specification for Concrete Aggregates). The saturated surface dry (SSD) bulk specific gravity was 2.68. Locally available 4.75 mm graded river sand conforming to ASTM C33 was used for this study. The fineness modulus and the SSD bulk specific gravity of sand were 2.79 and 2.59, respectively. A commercially available high-range water reducing admixture (HRWRA), conforming to ASTM C494, Type F (Specification for Chemical Admixtures for Concrete), was used in this study.

Table 1 Properties of the Materials Used

Materials	Slag [a]	Fly Ash
Specific gravity	2.88	2.47
Specific surface(m^2/kg)	580 (Blaine)	490 (Blaine)
Loss on ignition, %	0.06	3.00
SiO_2, %	36.0	49.34
Al_2O_3, %	12.0	22.73
CaO, %	42.0	3.09
MgO, %	6.0	1.06
SO_3, %	0.2	0.97
$Na_2O + 0.685 K_2O$, %	0.74	2.75
Fe_2O_3, %	1.8	16.01
Others, %	1.2	1.05

[a]The pH value (in water) for the slag is in the range of 10.5 ~ 12.7.

Mix Proportions

The details of the mix proportions and the selection procedures were described previously in details in Kar et al. (2013). The final mix proportions for AAB concrete are presented in Table 2 (reproduced from Kar et al., 2013).

3

Table 2 Final Concrete Mix Proportions for Alkali Activated Fly Ash and/or Slag

Precursor	Mixture Name	Fly ash	Slag	Sodium silicate (liquid)	Sodium hydroxide (solid)
		Kg/m^3	Kg/m^3	Kg/m^3	Kg/m^3
100 % Fly ash	FA 100	400	0	129.43	10.57
85% Fly ash + 15% slag	85/15	340	60	129.43	10.57
70% Fly ash + 30% slag	70/30	280	120	129.43	10.57
50% Fly ash + 50% slag	50/50	200	200	129.43	10.57
30% Fly ash + 70% slag	30/70	120	280	129.43	10.57
15% Fly ash + 85% slag	15/85	60	340	129.43	10.57
100% slag	SG 100	0	400	129.43	10.57
Pre blend 100% fly ash and solid NaOH for 15 days	FA 100 p15	400	0	129.43	10.57
Pre blend 100% fly ash and solid NaOH for 30 days	FA 100 p30	400	0	129.43	10.57
Pre blend 100% fly ash and solid NaOH for 60 days	FA 100 p60	400	0	129.43	10.57

Note: The quantity of coarse aggregate was kept constant at 1209 kg/m^3 and that of fine aggregate at 651 kg/m^3 for all mixes. The quantity of HRWRA used was in the range of 5060 ~ 6745 ml/m^3. The Ms modulus was 1.4 for all mixes.

Experimental Methods
Ultrasonic Pulse Velocity Measurements and Dynamic Modulus of Elasticity

The ultrasonic pulse velocity test is widely accepted as an efficient nondestructive test method to determine the velocity of longitudinal (compressional) waves. This technique consists of measuring the time taken by a pulse to travel a measured distance. The apparatus includes transducers which are kept in contact with the concrete specimen, a pulse generator with a frequency in the range of 10 to 150 kHz, an amplifier, a time measuring circuit, and a digital display of the time taken by the pulse of longitudinal waves to travel between the transducers through the concrete. The test was conducted as prescribed by ASTM C597 (Standard Test Method for Pulse Velocity through Concrete). The ultrasonic pulse velocities were obtained from tests on 75 mm × 75 mm × 275 mm (width × depth × length) prisms. The dynamic modulus of elasticity values were determined using cylinder specimens, 101.6 mm in diameter and 203.2 mm in length, as per ASTM C215 (Standard Test Method for Fundamental Transverse, Longitudinal, and Torsional Resonant Frequencies of Concrete Specimens).7-day, 28-day, and 90-day old specimens were studied for each mixture proportion. The tests reported below are similar to previous work of the same authors (Kar et al., 2013).

Compressive Strength Determination

Compressive strengths were measured in accordance with ASTM C39 (Standard Test Method for Compressive Strength of Cylindrical Concrete Specimens). Tests were conducted at 7, 28, and 90 days after casting, on 101.6 mm diameter and 203.2 mm long cylinder specimens. Three different temperatures: 23˚C (room temperature) and 40˚C, and 60˚C (the last two temperatures were obtained in an oven) were used to cure the respective specimens for 24 hours. The specimens were cured after 24 hours of casting for each of three different temperatures. Both curing time and curing temperature influence the compressive strength of AAB concrete specimens. Average values of compressive strength of 3 specimens for each mixture proportion were used for the present study. Another set of experiments were conducted to study the behavior of AAB concrete to gradually increasing compressive stress using the cylindrical test specimens mentioned above. The observations were recorded for the corresponding ultrasonic pulse velocities at definite intervals of gradually increasing compressive loads to an extent that the loading was stopped just before the specimens failed in compression. For each of the specimens, 0.9 f_c' (i.e. the compressive strength for that particular mixture proportion) was chosen as the limit to which they were loaded.

Results and Discussions

The results obtained from the different experiments are presented in this section and are used to make observations and conclusions about the characteristics of AAB concrete.It is observed that the compressive strength increased with increase in percentage of slag in the precursor. The AAB concrete specimens made with fly ash as precursor had the least compressive strength while the AAB concrete specimens made with slag as precursor showed the highest compressive strength for all three temperature levels. Preblending the fly ash with NaOH did not seem to have any influence on the compressive strength values. The increase of compressive strength with increasing curing temperature was observed for the AAB cube specimens as well as the AAB concrete cylinders. The variations of dynamic modulus of elasticity and compressive strength with ultrasonic pulse velocity are shown in the following sections. The relevant figures were published in Kar et al. (2013).

Variation of Dynamic Modulus of Elasticity with Ultrasonic Pulse

The wave velocity, v, in a homogeneous, isotropic and elastic medium is related to the dynamic modulus of elasticity, E_c, by the expression:

$$v^2 = \frac{E_c(1-\mu)}{\rho(1+\mu)(1-2\mu)} \tag{1}$$

Where ρ is density and μ is Poisson's ratio.
We can rewrite the eqn. (1) as

$$v^2 \propto E_c \tag{2}$$

Density and Poisson's ratio are constants for a particular specimen as the different specimens corresponding to each mixture proportion are assumed to be homogenous. Although, normal concrete violates the physical requirements for the validity of the above expression, Nilsen and Aitcin (1992) showed the usefulness of this technique in case of high strength concrete. Poisson's ratio varies within a small range of 0.16 to 0.25, leading to about 11% reduction in the computed values of the corresponding modulus of elasticity. So, the above technique can satisfactorily be used for field applications to estimate the modulus of elasticity from pulse velocity.

The experimental results for dynamic modulus of elasticity and the corresponding ultrasonic pulse velocity results are provided in Fig. 1. The experimental data are used to formulate equations through linear regression to predict the dynamic modulus values using ultrasonic velocity values as input parameter. The results show that the ultrasonic pulse velocities increased with the increase in modulus of elasticity. In general, higher values of modulus of elasticity were obtained at higher temperatures. Equations were obtained using 'R' for the variation of modulus of elasticity, E_c, with the square of the ultrasonic pulse velocities, v^2. Eqn. (2) shows that theoretically the linear relationship between v^2 and E_c can be represented by a straight line passing through the origin. But that requires a regression regime forcing intercept to be zero. Consequently, R^2 cannot be used as a measure of accuracy of the prediction model (Eisenhauer, 2003). Hence, the sum of squares due to errors (SSE) are used as a measure of accuracy, and models with and without intercepts were developed to test which form of the equation produces lesser SSE (Table 3).

Similar equations (with and without intercepts) are also obtained to express linear relationship between E_c and v. This provides a simpler form of the model. Relationships are obtained for each of the three curing temperatures and another set of equations are generated for all the mixture proportions taken together.
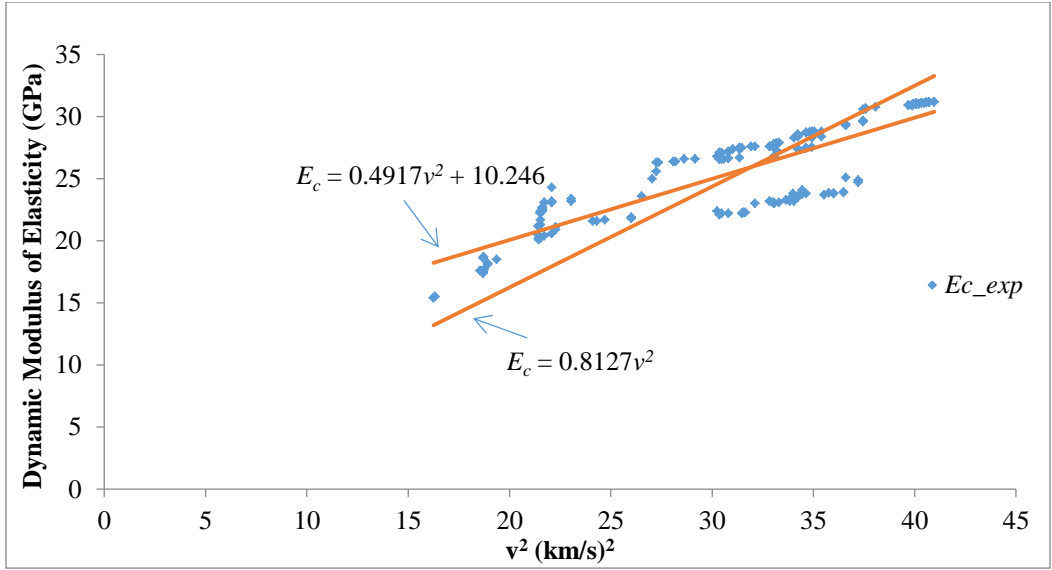
(a)
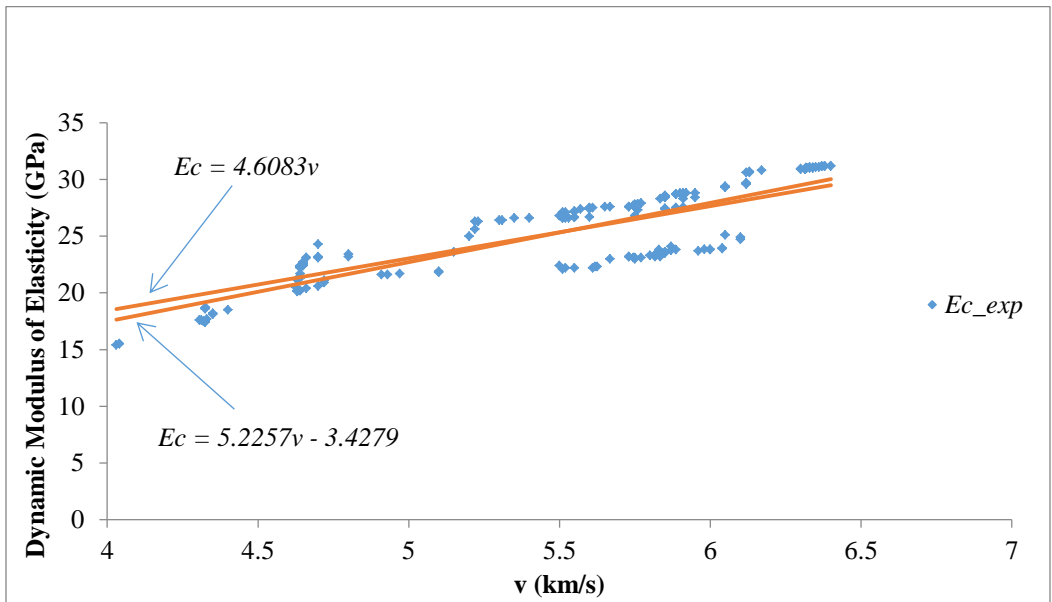
(b)

Fig. 1(a) Variation of E_c vs. v^2 for all specimens and (b) Variation of E_c vs. v for all specimens

The different equations for the cases mentioned above are provided in the Table 3, along with their corresponding SSE values.

Table 3 Variation of E_c vs. v^2 and E_c vs. v

Temperature	Equation without intercepts (SSE)	Equation with intercepts (SSE)
23°C	$E_c = 0.7390v^2$ (858.33)	$E_c = 0.3885v^2 + 10.451$ (61.51)
	$E_c = 4.0849v$ (48.92)	$E_c = 3.9565v + 0.5975$ (48.22)
40°C	$E_c = 0.8864v^2$ (495.52)	$E_c = 0.5478v^2 + 9.9034$ (56.86)
	$E_c = 4.8227v$ (73.44)	$E_c = 5.6706v - 4.5741$ (46.77)
60°C	$E_c = 0.8143v^2$ (289.52)	$E_c = 0.4211v^2 + 13.9520$ (17.38)
	$E_c = 4.8630v$ (20.72)	$E_c = 4.7722v + 0.5369$ (20.61)
All specimens	$E_c = 0.8127v^2$ (1703.69)	$E_c = 0.4917v^2 + 10.2460$ (775.63)
	$E_c = 4.6083v$ (800.65)	$E_c = 5.2257v - 3.4279$ (771.24)

Separate equations are developed for each curing temperature to understand the influence of the different curing temperatures. In case of unknown curing temperature during field applications, the general equation for all specimens can be utilized. For each of the cases, it is noticed that the equations obtained in case of E_c expressed as $f(v)$ shows lesser SSE values than the corresponding equations which expressed E_c as $f(v^2)$ in most cases. Also, inclusions of intercepts result into lower SSE values compared to the cases where intercepts are not considered.

Different sets of equations are obtained in order to express the relationship between the modulus of elasticity values and the ultrasonic pulse velocities, for each of the three different curing temperatures, as well as for all the specimens considered together. The last set of equations would be useful when the curing temperature is unknown. Engineers can use the ultrasonic pulse velocity values at different locations on structural elements to predict the modulus of elasticity. These values can be used to estimate the stiffness and integrity of the member.

Variation of Compressive Strength with Ultrasonic Pulse Velocity

The expression for the modulus of elasticity of concrete, E_c, in MPa units, recommended by ACI 318M-14 Metric Building Code Requirements for Structural Concrete and Commentary, for structural calculations, applicable to normal weight concrete, is

$$E_c = 4700\sqrt{f'_c} \qquad (3)$$

Where f'_c is the compressive strength of standard test cylinders in MPa units.

Rewriting,

$$f'_c \propto E_c^2 \qquad (4)$$

Combining eqns (3) and (4),

$$f'_c \propto v^4 \qquad (5)$$

The present study aims to correlate the compressive strength and the ultrasonic pulse velocity and use that correlation to predict compressive

strength values in the field. The load carrying capacity of the structure and the possibility of its deterioration due to cracks can be estimated.

The relationship between the modulus of elasticity and the compressive strength as mentioned earlier, holds good for PC concrete. As the present study deals with a different material, it is necessary to establish a different set of equations to describe the relationship between the modulus of elasticity and the compressive strength for this new material. The parameter that is measured in the field is the ultrasonic pulse velocity. The present study develops equations to express the modulus of elasticity as a function of the ultrasonic pulse velocity and also the compressive strength as a function of the ultrasonic pulse velocity. Theoretically, the modulus of elasticity is proportional to the square of the ultrasonic pulse velocity and the compressive strength is proportional to the fourth power of the ultrasonic pulse velocity. Hence the present study expresses $E_c = f(v^2)$ and $f_c' = f(v^4)$. However, if the predicted values of the E_c or the f_c' (determined by expressing them as functions of v) lies on the linear region of their respective curves, then E_c or f_c' will both be linearly correlated with v. As a result, the present study expresses $E_c = f(v)$ and $f_c'=f(v)$ in addition to the expressions already mentioned. The latter case was considered in order to obtain a simpler model. Also, Eqn. (5) shows that theoretically the linear relationship between v^4 and f_c' can be represented by a straight line passing through the origin. But that requires regression through origin and R^2 cannot be used as a measure of accuracy of the prediction model (Eisenhauer, 2003). Hence, the sum of squares due to errors (SSE) are used as a measure of accuracy, and models with and without intercepts were developed to test which form of the equation produces lesser SSE (Table 4).

Different graphs were obtained for the three different curing temperatures used in the study. In addition, another set of equations and graphs are provided in the case of the compressive strength data for all the specimens taken together irrespective of the curing temperature. This is of great use in predicting the compressive strength from the ultrasonic pulse velocity value when the curing temperature is unknown. The variations of the compressive strength with ultrasonic pulse velocities are presented in Fig. 2. The results showed that the ultrasonic pulse velocities increased with increasing compressive strength. In general, higher values of compressive strength were obtained at higher temperatures. The highest compressive strength was obtained for the 90-day age specimens cured at 60˚C for 24 hours.
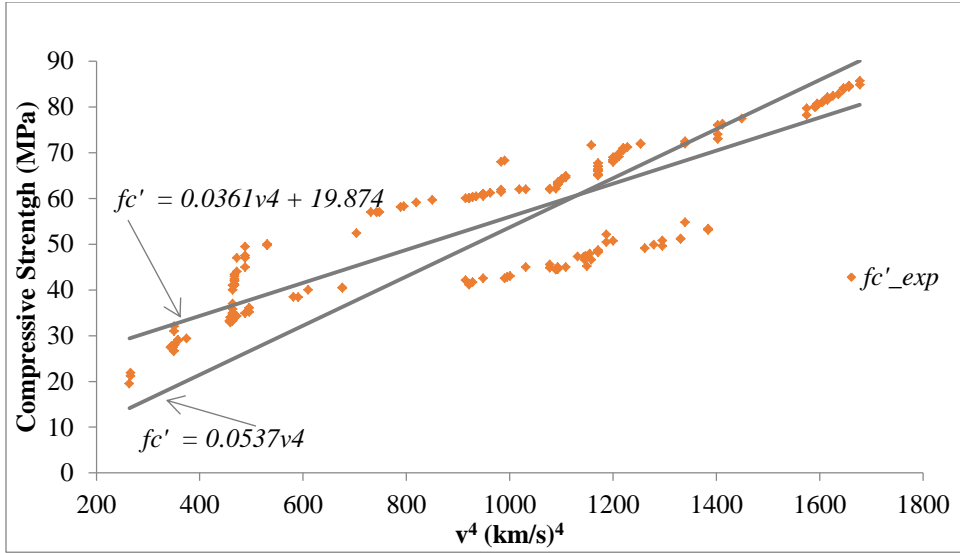
(a)
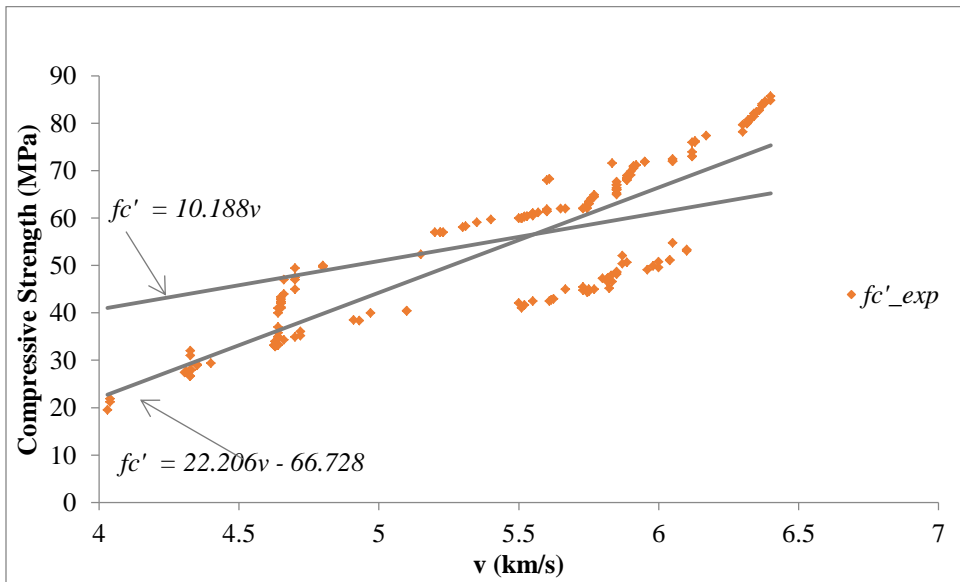
(b)

Fig. 2 (a) Variation of f_c' vs. v^4 for all specimens and (b) Variation of f_c' vs. v for all specimens

The different equations for the cases mentioned above are provided in Table 4, along with their corresponding SSE values.

Table 4 Variation of f_c' vs. v^4 and f_c' vs. v

Temperature	Equation without intercepts (SSE)	Equation with intercepts (SSE)
23°C	$f_c' = 0.0438v^4$ (4570.57)	$f_c' = 0.0235v^4 + 20.622$ (329.48)
	$f_c' = 7.7849v$ (1056.35)	$f_c' = 13.224v - 29.224$ (214.45)
40°C	$f_c = 0.0618v^4$ (4515.80)	$f_c = 0.0395v^4 + 21.245$ (736.83)
	$f_c' = 10.3708v$ (3735.58)	$f_c' = 22.7200v - 65.909$ (607.91)
60°C	$f_c' = 0.0550v^4$ (5208.10)	$f_c' = 0.0302v^4 + 32.947$ (186.60)
	$f_c' = 12.009v$ (1792.51)	$f_c' = 22.676v - 63.023$ (275.04)
All specimens	$f_c' = 0.0537v^4$ (23028.00)	$f_c' = 0.0361v^4 + 19.874$ (12506.59)
	$f_c' = 10.1883v$ (24225.75)	$f_c' = 22.2060v + 66.728$ (13080.24)

As in the case of modulus of elasticity, different equations were developed (with and without intercept) for each curing temperature in order to understand the effects of the different curing temperatures. However, if the curing temperature is unknown during field applications, then the user can utilize the general equation obtained for all specimens taken together. For each of the cases, it was noticed that the equations obtained in case of f_c' expressed as $f(v)$ showed lesser SSE values than the corresponding equations which expressed f_c' as $f(v^4)$ in most cases but not all the cases. Also, the equations with intercept resulted in lower SSE values compared to the corresponding equations without intercept.

Two different sets of equations were obtained in order to express the relationship between the modulus of elasticity values and the ultrasonic pulse velocities, for each of the three different curing temperatures, as well as for all the specimens considered together. The last set of equations would be useful if the curing temperature is unknown. In the field, it might be useful for the engineer to measure the ultrasonic pulse velocity at different locations on a structural element made out of the AAB concrete. The suggested equations can then be used to predict compressive strength at the corresponding locations. These values can be used to detect the presence of deterioration in the structure if some locations show low ultrasonic pulse velocities which will imply loss of compressive strength, and hence, the presence of deterioration. It was generally observed that the ultrasonic pulse velocity values had positive correlation with the compressive strength as well as the modulus of elasticity values. It was also observed that the ultrasonic pulse velocities decreased as the applied stress increased. Hence, it was concluded that if the measured ultrasonic pulse velocities were lower than the predicted values, it was an indication of deterioration in the structural element.

In order to determine the effect of compressive stress that has been exerted on the structure, the present study also investigated the variation of ultrasonic pulse velocity with applied compressive stress (σ_c) on AAB concrete specimens. The details are presented in the following section.

Effect of Gradually Increasing Applied Compressive Stress on Ultrasonic Pulse Velocity

The specimens used for this experiment were same as the 28-day old cylinders used for dynamic modulus of elasticity and compressive strength determination. Plots are made and equations are developed at each temperature to express σ_c as functions of v and v^4.

The results shows that the maximum ultrasonic pulse velocities were observed at zero applied stresses, i.e., when there was no deterioration. As the applied stress was increased gradually, the ultrasonic pulse velocities decreased appreciably. The lowest ultrasonic pulse velocities were observed when the applied stresses were the largest, i.e., when the concrete specimen was close to failure. Equations were obtained for the variation of applied strength, σ_c, with the fourth power of the ultrasonic pulse velocities, v^4, and then between σ_c and v, for each of the three curing temperatures. Another set of equations were generated for all the mixture proportions taken together, irrespective of the curing temperatures. Due to the nature of the plot between σ_c and v^4 (already published in Kar et al. (2013)), additional plots were drawn in the present study for $\ln(\sigma_c)$ versus v^4 to investigate if there was any improvement in the prediction equation in the case of all specimens considered together. For the sake of brevity, only the overall plots for variation of σ_c vs. v^4 and σ_c vs. v are provided (Figs. 3(a) through (c)). The different equations for the above cases are provided in Table 5, along with their corresponding R^2 values. The equations obtained in case of σ_c expressed as $f(v)$ showed better R^2 values than the corresponding equations which expressed $\ln(\sigma_c)$ as $f(v^4)$, which in turn showed better R^2 values than $\sigma_c = f(v^4)$.
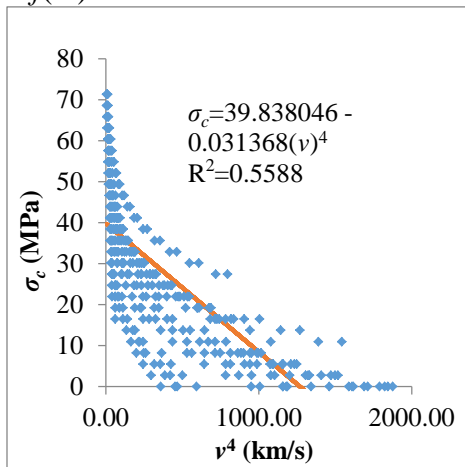
(a)
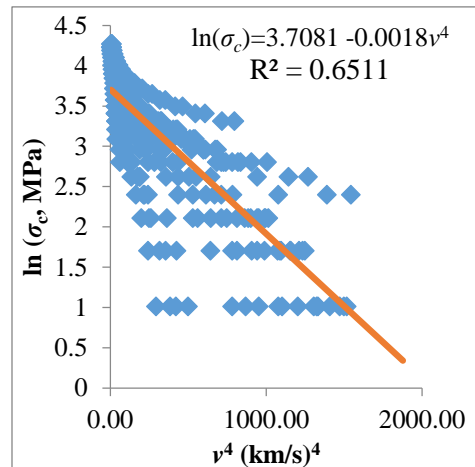
(b)
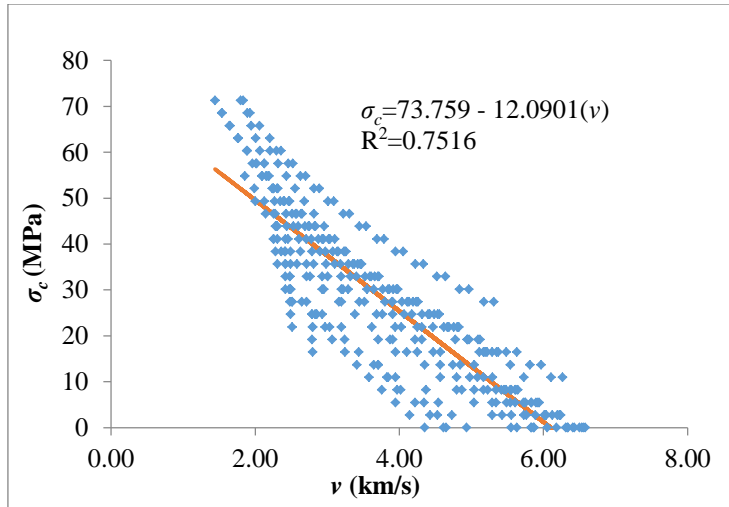
(c)

Fig. 3(a) Variation of σ_c vs. v^4 for all specimens; (b) Variation of $\ln(\sigma_c)$ vs. v^4 for all specimens and (c) Variation of σ_c vs. v for all specimens at 28 days

Table 5 Variation of σ_c vs. v^4 and σ_c vs. v

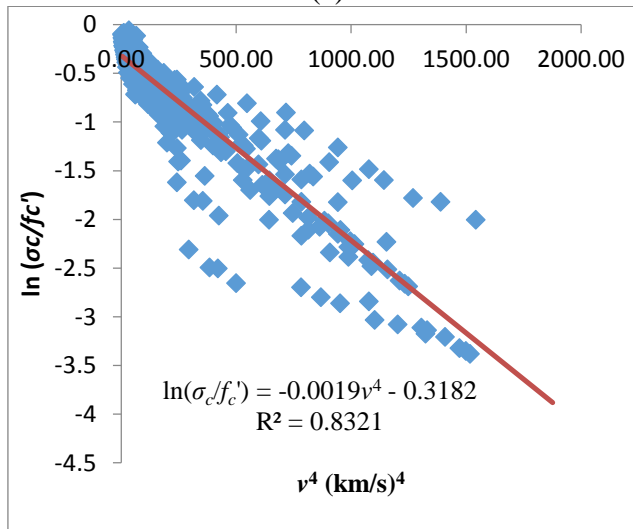| Temperature	Equation	R^2
23°C	$\sigma_c = 28.5419-.0282v^4$	0.5438
	$\sigma_c = 55.5818-9.807v$	0.7470
40°C	$\sigma_c = 38.9706-0.0311v^4$	0.6125
	$\sigma_c = 74.7488-12.1963v$	0.7777
60°C	$\sigma_c = 47.5657-0.0349v^4$	0.7182
	$\sigma_c = 83.1580-13.2371v$	0.9187
All specimens	$\sigma_c = 39.8380-0.0314v^4$	0.5588
	$\ln(\sigma_c)= 3.7081-0.0018v^4$	0.6511
	$\sigma_c = 73.7590-12.0901v$	0.7516

Subsequently, in order to find out the extent of loading, or what fraction of the compressive load has already been exerted on the structure, the present study looks at the ratio of the applied stress to the compressive strength ratio (σ_c/f_c') of the aforementioned 28-day old concrete specimens. Plots are made and equations are developed at each temperature to express σ_c/f_c' as functions of v and v^4.

The results shows that the maximum ultrasonic pulse velocities were observed when the σ_c/f_c' ratio was zero, i.e., at zero applied stresses. As the σ_c/f_c' ratio was increased gradually, the ultrasonic pulse velocities decreased appreciably. The lowest ultrasonic pulse velocities were observed when the σ_c/f_c' ratios were the largest, i.e., when the concrete specimen was close to failure. Equations were obtained for the variation of σ_c/f_c' ratio with the fourth power of the ultrasonic pulse velocities, v^4, as well as between σ_c/f_c'

ratio and v, at each of the three curing temperatures. Another set of equations were generated for all the mixture proportions taken together, irrespective of the curing temperatures. Due to the nature of the plot between σ_c/f_c' and v^4 (as furnished in Kar et al. (2013)), additional plot was drawn in the present study for $\ln(\sigma_c/f_c')$ versus v^4 to see if there was any improvement in the prediction equation in the case of all specimens considered together. For the sake of brevity, only the overall plots for variation of σ_c/f_c' ratio vs. v^4 and σ_c/f_c' ratio vs. v are provided (Figs. 4(a) through (c)). The different equations for the cases mentioned above are provided in Table 6, along with their corresponding R^2 values. The equations obtained in case of σ_c/f_c' expressed as $f(v)$ showed   better R^2 values than the corresponding equations which expressed $\ln(\sigma_c/f_c')$ as $f(v^4)$, which in turn showed better R^2 values than $\sigma_c/f_c' = f(v^4)$.

(a)

(b)

14
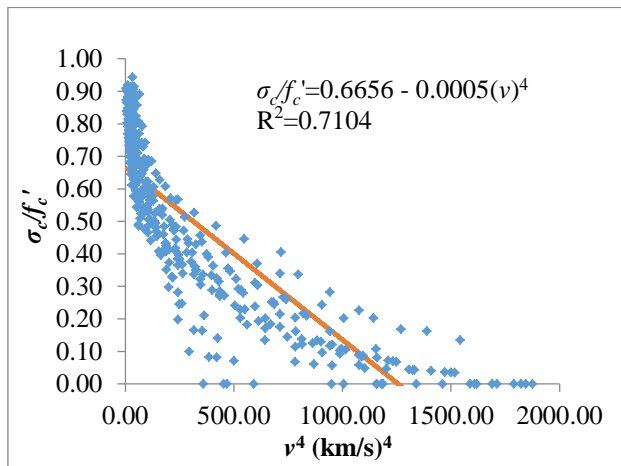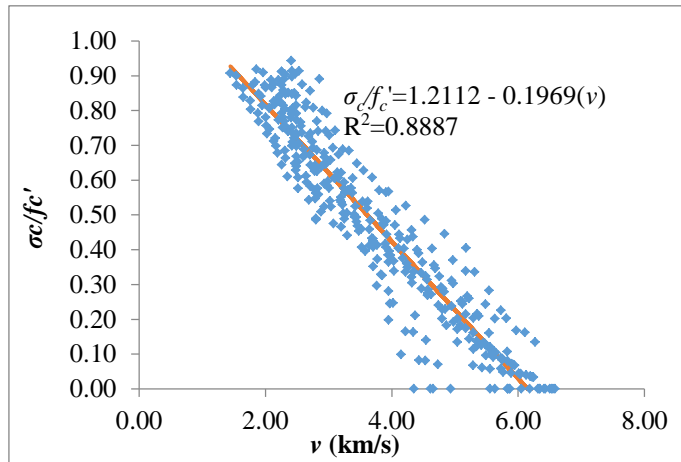
(c)

Fig. 4(a) Variation of σ_c/f_c' vs. v^4 for all specimens; (b) Variation of $\ln(\sigma_c/f_c$') vs. v^4 for all specimens and (c) Variation of σ_c/f_c' vs. v for all specimens at 28 days

Table 6 Variation of σ_c/f_c' vs. v^4 and σ_c/f_c' vs. v

Temperature	Equation	R^2
23˚C	$\sigma_c/f_c' = 0.6694-0.0007v^4$	0.6437
	$\sigma_c/f_c' = 1.2833-0.2263v$	0.8370
40˚C	$\sigma_c/f_c' = 0.6944-0.0006v^4$	0.7417
	$\sigma_c/f_c' = 1.3238-0.2161v$	0.9034
60˚C	$\sigma_c/f_c' = 0.6545-0.0005v^4$	0.7703
	$\sigma_c/f_c' = 1.1356-0.1798v$	0.9572
All specimens	$\sigma_c/f_c' = 0.6657-0.0005v^4$	0.7104
	$\ln(\sigma_c/f_c') = -0.0019v^4 - 0.3182$	0.8321
	$\sigma_c/f_c' = 1.2112-0.1969v$	0.8887

Conclusion

Based on the above studies the following conclusions are made:

1.   The ultrasonic pulse velocity increased with increasing dynamic modulus of elasticity. The modulus of elasticity was proportional to the square of the ultrasonic pulse velocity according to theory. The corresponding regressions through the origin would result in statistically erroneous results if the accuracies were measured in terms of R^2. Hence, prediction equations were developed with intercepts in the model. Linear relationships between modulus of elasticity and ultrasonic pulse velocities produced more accurate predictions.

2.   The compressive strength was found to be proportional to the fourth power of ultrasonic pulse velocity, but the linear correlation between compressive strength and ultrasonic velocity produced more accurate predictions. Regressions through the origin posed the same issues in this case

too as observed for the modulus of elasticity. Therefore equations developed with intercepts.

3.   The sum of squares due to errors (SSE) are used as a measure of accuracy, and models with and without intercepts were developed to test which form of the equation produces lesser SSE.

4.   The ultrasonic pulse velocities were found to be largest when the AAB concrete specimens were subjected to no stress. As the σ_c/f_c' ratio was increased gradually, the ultrasonic pulse velocities decreased appreciably. The lowest ultrasonic pulse velocities were observed when the σ_c/f_c' ratios were the largest, i.e., when the concrete specimen was close to failure.

5.   By normalizing the stress level (σ_c) of different AAB concrete with respect to their corresponding ultimate strengths (f_c'), a linear relationship was found to exist between the σ_c/f_c' ratio and the ultrasonic pulse velocity.

6.   This paper has shown that the ultrasonic pulse velocity technique can be effectively used to estimate the modulus of elasticity, compressive strength, and stress level of AAB concrete for wide range of mixes, curing temperature, and ages. This will help in monitoring the quality control and deterioration of the different AAB concrete structures in the field. Even in case of existing AAB concrete structures where curing temperature, ages, and AAB mix sources are not known, the present correlations can still be used to estimate the strength, modulus of elasticity, and stress level with reasonable accuracy.

Acknowledgements

References:

ASTM C33M-13 (Standard Specification for Concrete Aggregates), Annual Book of ASTM Standards, Vol. 04.02, Concrete and Aggregates, American Society for Testing and Materials, 2013.

ASTM C39/C39M-12a (Standard Test Method for Compressive Strength of Cylindrical Concrete Specimens), Annual Book of ASTM Standards, Vol. 04.02, Concrete and Aggregates, American Society for Testing and Materials, 2013.

ASTM C215-08 (Standard Test Method for Fundamental Transverse, Longitudinal, and Torsional Resonant Frequencies of Concrete Specimens),

Annual Book of ASTM Standards, Vol. 04.02, Concrete and Aggregates, American Society for Testing and Materials, 2013.

ASTM C494 Type F (Specification for Chemical Admixtures for Concrete), Annual Book of ASTM Standards, Vol. 04.02, Concrete and Aggregates, American Society for Testing and Materials, 2013.

ASTM C597-09 (C597-09 Standard Test Method for Pulse Velocity Through Concrete), Annual Book of ASTM Standards, Vol. 04.02, Concrete and Aggregates, American Society for Testing and Materials, 2013.

ASTM C618 (Standard Specification for Coal Fly Ash and Raw or Calcined Natural Pozzolan for Use in Concrete), Annual Book of ASTM Standards, Vol. 04.02, Concrete and Aggregates, American Society for Testing and Materials, 2013.

ASTM C989 (Standard Specification for Slag Cement for Use in Concrete and Mortars), Annual Book of ASTM Standards, Vol. 04.02, Concrete and Aggregates, American Society for Testing and Materials, 2013.

Davidovits, J., "Geopolymers of the First Generation: SILIFACEProcess". In: Davidovits, J., Orlinski, J. (Eds.), Proceedings of the 1st International Conference on Geopolymer '88, Vol. 1, Compiegne, France, 1–3 June, pp. 49–67 pp., 1988.

Davidovits, J., "Geopolymers: Inorganic polymeric new materials", Journal of Materials Education, Vol. 16, pp. 91–139 pp., 1994.

Davidovits, J., "30 Years of Successes and Failures in Geopolymer Applications. Market Trends and Potential Breakthroughs.", Geopolymer 2002 Conference, October 28-29, 2002, Melbourne, Australia, 2002

Eisenhauer, J. G.,"Regression through the Origin", Teaching Statistics, Vol. 25, No. 3, 76 – 80 pp., 2003

Kar, A., Halabe, U. B., Ray, I., & Unnikrishnan, A., " Nondestructive Characterizations of Alkali Activated Fly Ash and/or Slag Concrete.", European Scientific Journal, Vol. 9, No. 24, 52 – 74 pp., 2013

Nilsen, A. U. and Aitcin, P.-C., "Static modulus of elasticity of high-strength concrete from pulse velocity tests", Cement, Concrete and Aggregate, Vol. 14, No. 1, 64 – 66 pp., 1992.

Provis, J. L. and van Deventer, J. S. J., Geopolymers: structure, processing, properties and industrial applications, Publisher: Oxford: Woodhead ; Boca Raton, FL : CRC Press, 2009.